CHAPTER 3

DESIGN AND FABRICATION OF RIGS FOR SPECIMENS PREPARATION AND TESTING

3.1 Introduction

In this chapter, the discussion focuses on the rigs used for specimen preparation, experimentations and final load tests. The detailed focuses on the design and development of sustainable stressed rig that was used for this study programme. The function of other developed and fabricated rigs is also briefly discussed in this chapter.

3.2 The Significant of Rigs and Fixtures Design Development

The objective of developing and fabricating rigs for specimen preparation, experimentation and load test in this study programme was to produce reliable mechanical rigs able to perform and produce consistent results.

3.2.1 Specimen Preparation Rigs and Fixtures

In this study programme, there were three types of mechanical rigs and fixtures that were developed and fabricated to fulfil the research programme needs, namely;

i. CFRP plate end tabs bonding rig
ii. Epoxy adhesive specimen mould fixture
iii. CFRP plate-epoxy-concrete prism bonding rig and fixture

3.2.1.1 CFRP Plate End Tabs Bonding Rigs

There were two types of rigs fabricated to serve for different specimen preparation needs. They are as follows;

i. Rig for bonding aluminium end tabs to CFRP plate specimen (Fig. 3.1).
ii. Rig for bonding mild steel end tabs to CFRP plate specimen (Fig. 3.2).

Both rigs were very significant in producing specimens with high dimensional accuracy and consistency. The process of bonding aluminium and mild steel end tabs to CFRP plate was using structural epoxy system. The epoxy system was in the form of paste. The application of this epoxy system needed a strict procedure to perform as stated by the manufacturer specifications.

Both rigs shown in Fig. 3.1 and Fig. 3.2 were designed and developed to accommodate ten and five units of CFRP Plate specimens, respectively, in a single operation. Both of them were made from mild steel material and were provided with pressure plates that were mechanically controlled by screws. This was to provide a uniform pressure and to be able to control the adhesive thickness accordingly. The specimens were left for curing within 24 hours before being demoulded from the rigs. The detailed operation for both rigs can be referred to in Chapter 4 and Chapter 6.

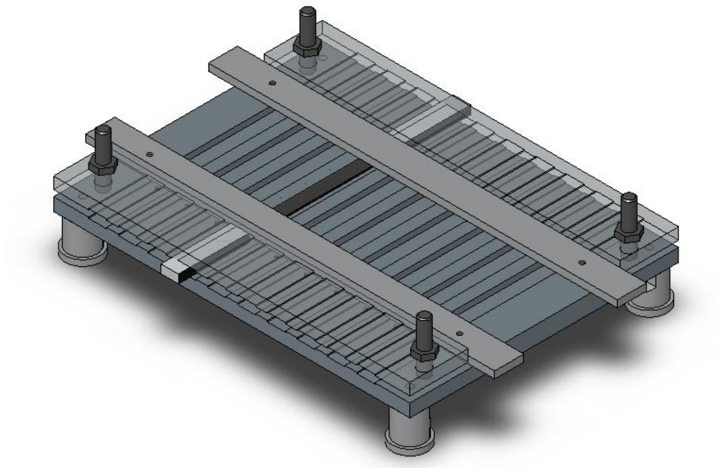

Fig. 3.1: Rig developed for bonding aluminium end tabs to CFRP plate specimen

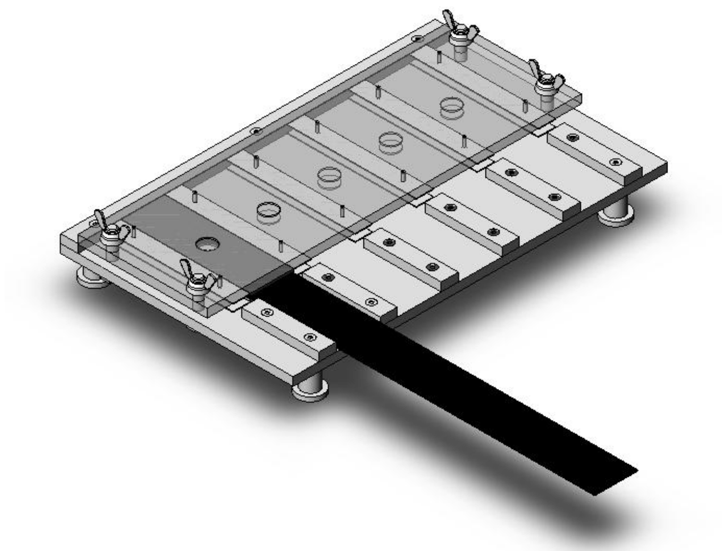

Fig. 3.2: Rig developed for bonding mild steel end tabs to CFRP plate specimen

3.2.1.2 Epoxy Specimen Mould Fixture

Due to various technical problems, the mould was eventually successfully developed and fabricated under several development stages. The problem started from the difficulty in handling the epoxy form, i.e. highly viscosous (paste like) during moulding and also in difficulty of demoulding the cured cast epoxy due to their brittleness. The epoxy system needed to be handled in a very careful manner and required skilled operator to perform the tasks. The short pot life was another constraint that was faced during the operation.

The fabricated mould consisted of male and female (i.e. closed mould system), made of mild steel and used several screws for tightening purposes. A metal block was used on top of the male mould as a weight to produce a static pressure. In one casting operation, the mould was capable of producing ten units of cast epoxy specimens. The specimens were left in the mould for at least 24 hours to be permanently cured. The detailed operation of specimen preparation moulding fixtures can be referred to in Chapter 5.

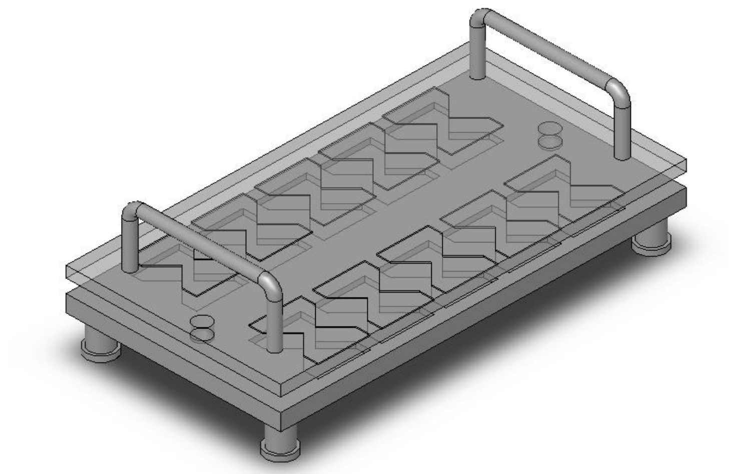

Fig. 3.3: Closed type mould developed and fabricated for epoxy butterfly shape specimen preparation

3.2.1.3 CFRP Plate-Epoxy-Concrete Prism Bonding Rig and Fixture

The rig for preparing bonded specimen of CFRP-epoxy-concrete prism was developed through various studies especially in considering the specimen alignment, adhesive thickness and bonding operation. The difficulty in controlling the uneven concrete prism cross-section was the main concern in bonding operation. Fig. 3.4 shows the final rig development which was equipped with supporting components that were able to perform the bonding and maintain the alignment. The rig was also provided with pressure plate used to control the quality of bonding and the adhesive thickness, two side plates to control the alignment of the concrete prism and a slot to control the CFRP plate alignment. Screws were used to lock the pressure plates onto the specimen during operation. The detailed operation of the rig can be referred to in Chapter 6.

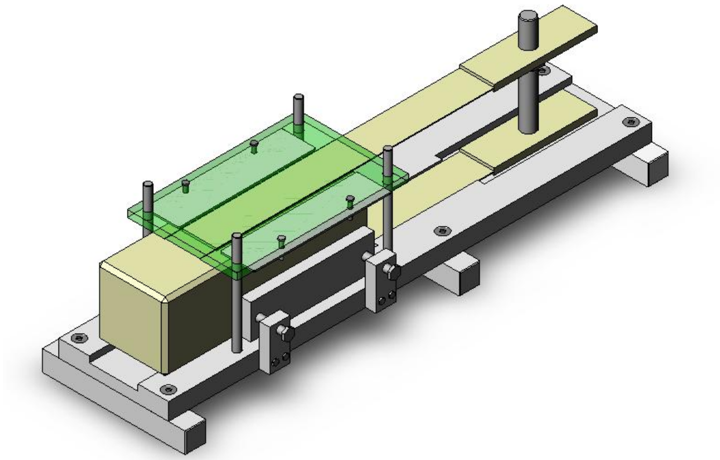

Fig. 3.4: The final development of CFRP plate-epoxy-concrete prism bonding rig

3.3 Shear Load Test Fixture

The test rig was known as Arcan fixture and was first introduced in 1978. The test fixture was developed to overcome problems such as the existence of unwanted stress components, such as tensile stress besides the shear stress in the final measurement. In order to produce a uniform state of plane-stress for the solid specimen, Arcan *et al.* [62] was successful in developing this fixture to determine the mechanical properties of isotropic as well as orthotropic FRP composite materials under uniform plane stress conditions by means of a specially designed butterfly-shaped specimen as previously shown in Fig. 2.42 (Chapter 2).

From the literature study, it shows that previous researchers have developed fixtures based on their limitation in specimen or materials physical properties. In order to produce a reliable fixture that was able to produce better test results and to accommodate the brittle epoxy specimen in the study programme, the design development took into account all the problems faced from the first concept introduced by Arcan *et al.* [61] up to the most recent development by Yen *et al.* [63].

In principal, the test rig worked when the loading machine applied a tensile load onto the Arcan fixture through holders prior to the loading configuration being changed to shear mode and finally imposed onto the specimen. The direction of principal shear then acted in the direction of $\pm 45^{\circ}$ as referred to the horizontal axis of specimen significant section. The fixture holders were attached to the loading machine by two pins with a diameter of 15 mm. After the holder were attached to the loading machine, the complete Arcan grip fixture consisting of the butterfly specimen was connected to the holders by using two pins at the upper and lower sections of the fixture.

The schematic diagrams of developed and fabricated fixture are shown in Figs. 3.5 (a) and (b). Due to the brittleness of the specimen, the specimen was mounted and bonded using adhesive film into butterfly groove shape that was precisely built according to the specimen geometry. This operation could prevent the specimen from slipping during loading. The overall development of the rig was made from mild steel and was coated to prevent it from corroding. The speciality of this rig compared with previous constructions was the ability to produce perfect alignment under tensile loading configuration by double plate system construction. Using this technique, the effect of eccentricity which produced unbalanced moment could be eliminated.

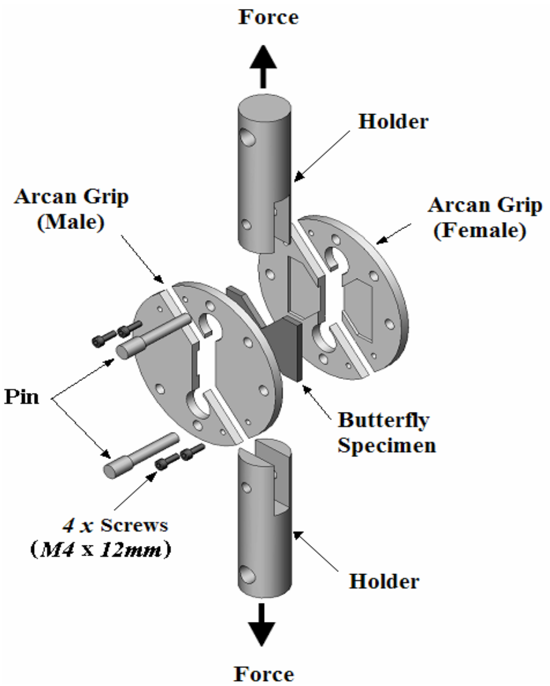

(a)

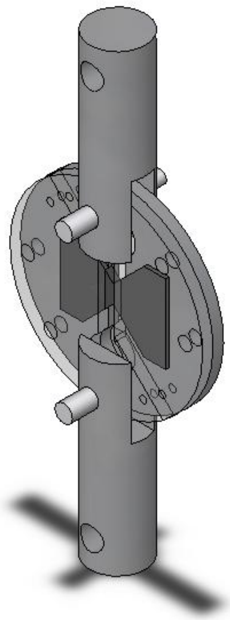

(b)

Fig. 3.5: Modified Arcan fixture used for this study programme (a) assembly form and (b) complete assembly form

3.4 CFRP Plate-Epoxy-Concrete Prism Pull-out Test Rig

The first of this type of rig construction was used by Swamy *et al.* [20] to study the effect of various adhesive thicknesses on the bond characteristics of mild steel plate bonded to concrete prism in 1986. Two pieces of steel plates 60 mm *x* 3 mm thick were bonded to the concrete prism 60 mm *x* 60 mm *x* 150 mm. The mild steel plates were subjected to tension through the designated arrangement of the test rig parts and then finally attached to the loading machine. In 1998, Mukhopadhyaya *et al.* [10] continued using the same test rig arrangement (Fig. 3.6) for bond durability study of GFRP plate bonded to concrete prism by focusing on the effects of different concrete mixed under aggressive exposure conditions.

In this study programme, the rig was designed, fabricated and assembled in the laboratory, specifically for this test, which was then fitted into a 100 kN Instron Universal Testing Machine. The compressive static force on the concrete prism was applied by means of a roller bearing, 75 mm wide. The tensile force applied to both

CFRP plates by means of a holder attached to the loading machine. Both CFRP plates were attached to the holder by means of pin connection and were prevented from lateral movement by fixing bolts and nuts.

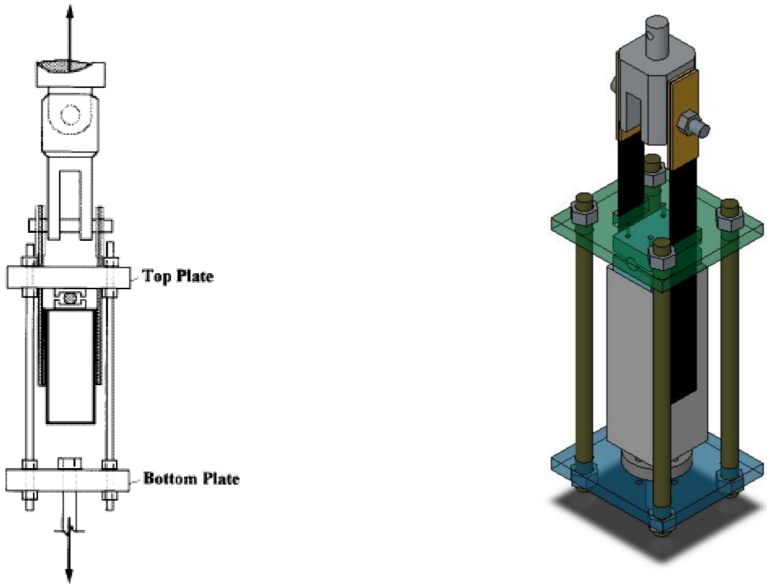

(a) (b)

Fig. 3.6: (a) The schematic diagram of pull-out test rig used by Mukhopadhyaya *et al*. [10] and (b) The final development of pull-out test rig for this study programme

3.5 The Sustainable Loads Experimentation Rig for CFRP Plate-Epoxy-Concrete Prism

The most significant objective in designing and manufacturing this rig was to create, transfer and sustain the tensile-shear-compressive loads imposed onto the CFRP plate-epoxy-concrete prism bonded specimen for bond durability experimentation assessment under stress. In order to achieve the design requirements and needs, important technical inputs and constraints were highlighted during the design process, and they are as follows;

i. applied load and loads transfer
ii. system equilibrium
iii. load sustainability
iv. accessibility and workability

3.5.1 Design Elements

In normal design practice, the most critical stage was to identify the needs of the design. In designing the load sustainable rig for the purpose of experimentation, the first problem to look into was the specimen geometry and configuration. After the problem been identified, a few design concepts were produced. The concepts should be able to solve problems such as identifying and selecting the suitable loading mechanism, load transducer, rig configuration and geometry. In the early stage, two loading mechanisms were identified, i.e. coil spring and mechanical jack. They were tested to investigate their loading capability, reliability and suitability. Unfortunately, the two loading mechanism failed to meet the design requirement due to the limitation on loading capability and geometrical constraint.

3.5.2 Problem Identification

In principal, the geometries and loading configuration imposed onto the specimen have been identified from various past researches related to studying bond characteristics of FRP or steel plate-concrete bonded system. Nakaba *et al.* [62] in their literature have listed methods that were commonly used to study bond characteristics, i.e. bending, single face shear, inserted, direct tensile and double face shear types. From those methods, double face shear was the most preferred and able to provide a significant bond test results. These were proven by the research works conducted by Swamy *et al.* [20], Mukhopadhyaya *et al.* [10], Nakaba *et al.* [54], Maeda *et al.* [74], Brosens and Van Gemert [73], Horiguchi and Saedki [23] and Toutanji and Ortiz [24].

The specimen's loading configuration that was previously used by Swamy *et al.* [20] and Mukhopadyaya *et al.* [10] was designed in such a way that the respected specimen's material strength properties could be exploited. By referring to the specimen's loading configuration shown in Fig. 3.7(a), it can be seen that the CFRP plates were designed to be subjected to tension and concrete prism to be in compression modes. The effect of relative loading configuration of both materials has produced shearing effect on both adherends bond interface and epoxy adhesive is shown in Fig. 3.7(b). By eliminating the effect of peeling stresses, another important design element, this kind of configuration represented the actual condition at FRP-concrete interface due to flexural loading of RC members that were externally bonded with FRP. This loading configuration was adopted and used in this study programme for unstressed and sustained load case of CFRP plate-concrete bonded system exposed to tropical environmental conditions.

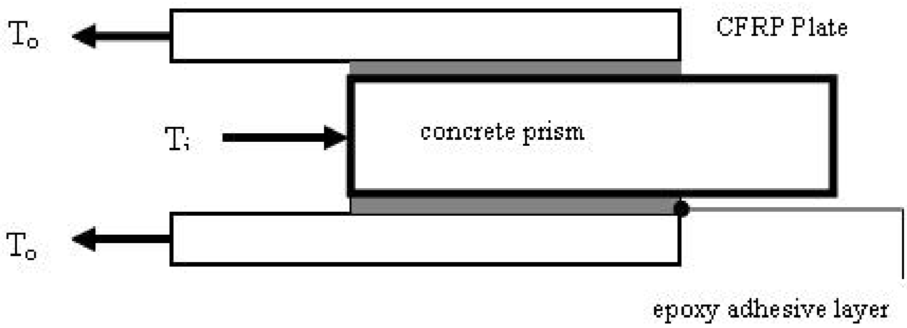

Fig. 3.7(a): Loading configuration for the CFRP Plate-Concrete Prism under Tension-Compression loading configuration

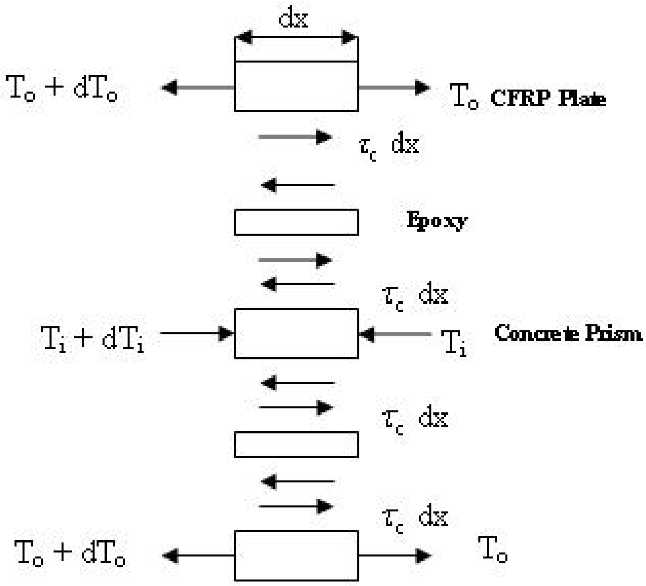

Fig. 3.7 (b): Elementary force analysis

3.5.3 Design Concept and Force Analysis

The force acting on each rig component was created by the compressive load produced by hydraulic force. The maximum compressive load produced by the pump was 50 kN. Then, the load from the pump was transferred to the upper and lower constrain plates before being distributed to other rig sub-components and specimen materials.

The point load from the upper plate was transferred to the bearing block and upper rod. Concrete received compressive load from the lower plate. The load that has been transferred to CFRP plate was in tensile and the steel tie rod experienced a compressive stress just after the hydraulic load has been released to zero.

3.5.4 Rig-Specimen Loading Analysis

The assumption made in the static load analysis was that the rig and the specimen were in equilibrium condition. The design calculation started with first identifying the most critical rig components and specimen material (i.e. specimen area directly subjected to applied load). The following are the rig components and candidate specimen under critical load-stress condition, namely;

i. pin (geometry and shear properties)
ii. tie rod (geometry, buckling and torque analysis)
iii. CFRP plate-mild steel end tab bonded area (failure analysis at loaded pinhole)

3.5.4.1 Pin Shear Failure Analysis

This failure mode was caused by high shear stresses in pin/bolt under bending load. From Fig. 3.8, it can be observed that the pin was critically in shear rather than in bending (safe in bending due to the load being transferred and distributed to bearing block). It was assumed the pin acting on the bearing block was subjected to point load and simply supported at both ends (i.e. conservative design).

By taking the value of yield strength for a high tensile steel as S_y = 460 N/mm^2 (BS 4449), the allowable shear strength, τ_{all} of pin could be determined from Mechanical Engineering Design Handbook [68] as follows,

$$\tau_{all} = 0.4S_y = 0.4(460)\ \text{N/mm}^2$$

In order to ensure that the pin/bolt did not fail in shear, the shear strength should be less or equal to pin allowable shear strength, $\tau_s \leq \tau_{all.}$

$$\tau_s \leq 0.4S_y = 184\ \text{N/mm}^2$$

By limiting the design applied load, P_{app} to 50 kN and the pin diameter was fixed to 20 mm, therefore, from the shear diagram, the calculated shear force was V = 25 kN, gives;

$$\tau_s = V/A_{pin/bolt} = 25 \text{ x } 10^3/[(\pi \text{ x } 20^2)/4]$$

$$\tau_s = \underline{\mathbf{79.60\ MPa}}$$

and finally,

$\tau_s < \tau_{all}$ **(therefore the pin was safe in shear)**

3.5.4.2 Pin Validation Test

The three-point bending test has been conducted on three bolt/pin specimens in order to determine the maximum deflection. The objective of the test was to validate the pin strength properties under bending load. The test results have shown that the maximum deflection of the pin was about 4.84 mm under bending load of 96 kN. The curve of load versus deflection is shown in Fig. 3.8. It can be observed that at 50 kN load level, the pin midpoint deflection was about 1.7 mm. The result was considered to be conservative due to the pin being uniformly supported along most of its length.

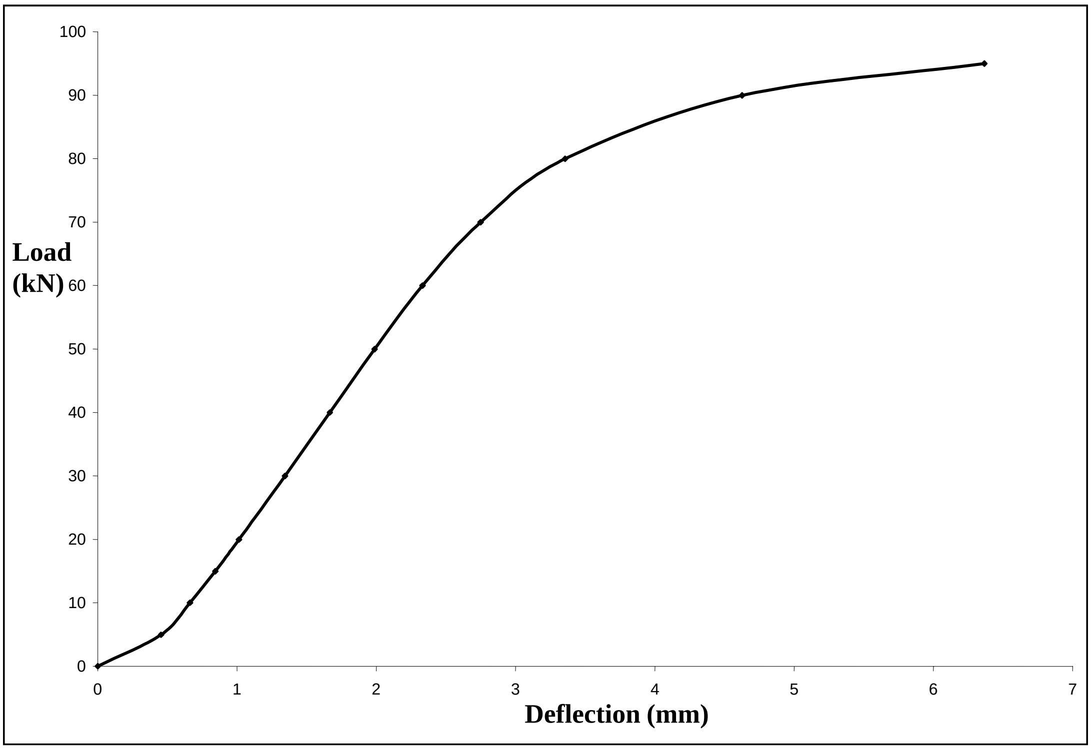

Fig. 3.8: Graph of load versus midpoint deflection of high tensile pin

3.5.4.3 Tie Rod Loads Analysis

The objective of analysis was to determine the geometries (i.e. length and diameter) of the high tensile steel tie rod that able to sustain the imposed design service load. The design load was fixed at 25 kN for each rod. The analysis was divided into determining the rod diameter and the rod critical length due to buckling effect (elastic instability).

i. Tie Rod Diameter

The applied load, P_{app} imposed onto the rod cross-sectional area, A_s was uniaxial compressive load. By assuming that the compressive strength, σ_c of the rod was equal to the tensile yield strength, $\sigma_{y,t}$ therefore, from Hooke's law;

$$\sigma_c = P_{app}/A_s \qquad [3.1]$$

Assuming, $\sigma_c = \sigma_{y,t}$ = 460 MPa and by taking safety factor of 1.5, gives, σ_c = 307 MPa. therefore, the diameter of the rod, d_t can be determined as follows,

$$d_t = \sqrt{(4P_{app}/\pi\ \sigma_c)}$$
$$= \sqrt{(4 \times 25 \times 10^3)/(\pi \times 307)}$$
$$= \underline{\mathbf{10.20\ mm}}$$

Therefore, the available standard size of 25 mm outside diameter was selected. The size selected also took into account the effect of aggressive exposure conditions such as salt water environment.

ii. Tie Rod Buckling Effect

This analysis was done to ensure the elastic stability of the tie rod (i.e. short column) subjected to axial compressive load. By using Euler's analysis, which assumed that the rod was perfectly straight, loaded precisely axial, the rod material was homogenous and stressed within linear elastic range. From Euler's [75] classical equation;

$$P_{cr} = \pi^2 EI/L_e^2 \qquad [3.2]$$

where,

P_{cr} = critical compressive load (N)
E = modulus of elasticity (MPa)
I = moment of inertia of the cross-section, A with respect to the buckling-bending (mm^4)
L_e = equivalent length of column (mm)

By substituting $I = A\rho^2$ into equation [3.2], gives;

$$S_{cr} = P_{cr}/A = \pi^2 E/(L_e/\rho)^2 \text{ or } S_{cr}/E = \pi^2/(L_e/\rho)^2 \qquad [3.3]$$

where,

L_e/ρ = slenderness ratio

By assuming the tie rod will be fixed at both ends, $L_e = 0.65L$ (minimum AISC recommend), therefore, $L_e = 0.65 \times 210$ mm = 136.5 mm

From equation [3.3],

$$S_{cr} = (25 \times 10^3 \times 4)/[\pi \times (24)^2]$$
$$= \underline{\mathbf{55.26\ MPa}}$$

Slenderness ratio for solid rod, $L_e/\rho = 136.5/(24/4)$, where, $\rho = D/4$

Therefore, $L_e/\rho = 1.42$, from S_{cr} versus L_e/ρ curves in [75] it could be concluded that the tie rod was highly elastically stable.

iii. Determination of Torque

The objective of this analysis was to determine the torque that should be applied to the rig's tie rods (power screws) nuts just after specimen stressing load reached their final target value. This was important to ensure that rig was able to sustain the load in a long period of time under various exposure conditions.

By considering the system shown in Fig. 3.9 was in equilibrium, the formulation involved in determining the torque that was used to tighten the screw are shown by the following equations;

For raising the load,

$$\sum F_H = P_R - N\sin\lambda_L - fN\cos\lambda_L = 0 \qquad [3.4]$$

$$\sum F_V = F + N\sin\lambda_L - N\cos\lambda_L = 0 \qquad [3.5]$$

Finally, to tighten (raising the load) the screw, the following equation [3.6] was used [76];

$$T_R = \frac{Fd_m}{2}\left[\frac{l + (\pi\, fd_m \sec 30^{o})}{(\pi d_m - fl \sec 30^{o})}\right] \qquad \textbf{[}3.6]$$

where,

Screw diameter, d = 24mm

Pitch, p = 3mm

Coefficients of friction, f = 0.15

Pitch diameter, d_m

Lead, l

Lead angle, λ_L = 30º

Thread type, n =2 (double thread)

The pitch diameter or mean diameter,

d_m = d-0.649519p

= 24-0.649519(3)

= **<u>22.05 mm</u>**

The lead,

$l = np$

l = 2(3) = 6mm

By limiting the load imposed on each tie rod as F = 25 kN, therefore the torque, T to turn or tighten the screw against the load is;

$$T = \frac{25(22.05)}{2}\left[\frac{6 + \pi(0.15)(22.05)(\sec 30^{o})}{\pi(22.05) - (0.15)(6)(\sec 30^{o})}\right]$$

***T* = <u>72.7 Nm</u> (Let's take 80 Nm as standard torque)**

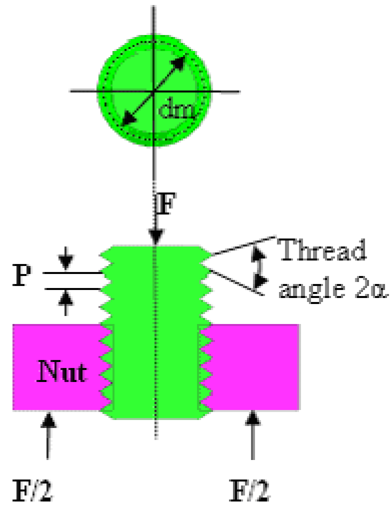

Fig. 3.9: Portion of power screw

3.5.5 CFRP Plate-End Tab Bond Failure Analysis

The stresses being built-up along the bonded area of CFRP plate and mild steel end tabs were the critical factors to be seriously considered in the overall rig design performances. This was to ensure the specimen did not fail in the clamping region rather than in the CFRP plate-concrete bonded area. The application of mild steel plate as end tabs was to prevent or to overcome the weakness of highly orthotropic properties of CFRP plate under tensile load during stress. Mukhopadhyaya *et al.* [10] in their experimental study of GFRP plate-concrete specimen had used mild steel plate geometry of 150 mm *x* 90 mm *x* 1.2 mm that was bonded on both side of GFRP pultruded plate. The use of mild steel plate was to ensure that the GFRP plate did not tear off prematurely due to weak and reduced cross section of the drilled hole. No sign of failure along the bonded area of GFRP plate-mild steel end tabs bonded area was reported in their study.

The objective of this analysis was to investigate the ultimate limit state of the bond joint of mild steel end tabs to CFRP plate under tensile load. The analysis focused on the stresses that occurred around pinhole and also along the bonded length of the specimen.

3.5.5.1 CFRP Plate Bonded with Mild Steel End Tabs Failure Analysis

In predicting the failure load, it was necessary to use both equilibrium and compatibility conditions. If perfect bond between CFRP plate and mild steel end tabs was assumed, then the CFRP plate and mild steel would have the same strain. Therefore, the applied tensile load, P_{app} was the summation of loads carried by the CFRP plate load, P_{cfrp} and the mild steel end tabs load, P_{steel} along the bonded area and could be shown by the following equation:

$$P_{app} = P_{cfrp} + P_{steel} \qquad [3.7]$$

If failure occuring along the bonded area was dominated by either shear-out or bearing or net-section or combination of them, of the CFRP plate, the following equation would be used to predict the total failure load, $P_{ult} = P_{app}$. Therefore,

$$P_{ult} = P_{cfrp,s} + P_{steel} \text{ if } P_{cfrp,s} < P_{cfrp,b} < P_{cfrp,n} \qquad [3.8]$$

$$P_{ult} = P_{cfrp,b} + P_{steel} \text{ if } P_{cfrp,b} < P_{cfrp,n} < P_{cfrp,s} \qquad [3.9]$$

$$P_{ult} = P_{cfrp,n} + P_{steel} \text{ if } P_{cfrp,n} < P_{cfrp,s} < P_{cfrp,b} \qquad [3.10]$$

Where CFRP plate shear load, $P_{cfrp,s}$, CFRP plate bearing load, $P_{cfrp,b}$ and CFRP plate net-section load, $P_{cfrp,n}$ could be determined by using equations [3.11], [3.12] and [3.13] that were referred to [77]. The least value provided by those equations would be used to predict the ultimate failure load acting at the highly stressed pinhole of CFRP plate-mild steel end tabs. By taking the value of CFRP plate shear strength, $\tau_{sn,k}$ as 50 MPa [70], therefore;

$$P_{cfrp,s} = \tau_{sn,k} \, x \; d_h \, x \, t \, / \, (k_s^1) \qquad [3.11]$$

$$= (50 \, x \, 20 \, x \, 1.6)/(0.45)$$

$$= \underline{\mathbf{3.556 \ kN}}$$

and

by taking the value of CFRP plate radial strength in 0º direction, $\sigma_{r,k}$ as 2,400 MPa (referred to CFRP plate tensile test data in Chapter 4), therefore;

$$P_{cfrp,b} = \sigma_{r,k}\ x\ (d_h\ x\ t)/(\ k_r^1) \quad [3.12]$$
$$= (2{,}400\ x\ 20\ x\ 1.6)/(1.3)$$
$$= \underline{\mathbf{59.08\ kN}}$$

and

by taking the value of CFRP plate tensile strength, $\sigma_{r,k}$ as 2,400 MPa (referred to CFRP plate tensile test data in Chapter 4), therefore;

$$P_{cfrp,n} = \sigma_{t,k}\ x\ (d_h\ x\ t)\ /(\ k_t^1) \quad [3.13]$$
$$= (2{,}400\ x\ 20\ x\ 1.6)/(1.6)$$
$$= \underline{\mathbf{48.00\ kN}}$$

and

by taking the value of allowable mild steel bearing stress, τ_B = 225 MPa (i.e. $0.9S_y$), give;

$$P_{steel} = 2\ x\ \tau_B\ (d_h\ x\ t) \quad [3.14]$$
$$= 2\ x\ 225\ x\ (20\ x\ 3)$$
$$= \underline{\mathbf{27.00\ kN}}$$

and, finally it is shown that $P_{cfrp,s} < P_{cfrp,b} < P_{cfrp,n}$ and therefore, P_{ult} is equal to as follows;

$$P_{ult} = P_{cfrp,s} + P_{steel}$$
$$= 3.56\ kN + 27.00\ kN$$
$$= \underline{\mathbf{30.56\ kN}}$$

3.5.6 Tensile Test for CFRP Plate Bonded with Mild Steel End Tabs

The objective of conducting the tensile test on CFRP plate -mild steel end tabs bonded system as shown in Fig. 3.10 was to identify the load limit that able to sustain when the real CFRP plate bonded to concrete prism been subjected to pull-push loading configuration.

Fig. 3.10: Test set-up for determination CFRP plate-mild steel end tabs bond strength

3.5.6.1 Performance Test Results

From Fig. 3.11, it can be seen that the local strain distribution along end tabs bonded length experienced compression (upper zone) and tension (lower zone). The maximum tensile load applied was about 35 kN before the specimen final failure mode started with CFRP plate shear out and debonding of mild steel end tabs at tensile bond region (right part). The weakness of shear properties in CFRP plate fibre-matrix system was the main factor that initiated the failure around end tabs bond region. Debonding of mild steel end tab from CFRP plate was due to excessive local bond stress that was developed at specimen loaded end in tensile region. At around the pin hole region, it could be seen that the bearing stress concentrated at the compression region (left part). The maximum local strain was concentrated at the regions of 45°, 315° and 0° directions. The maximum failure strain was about -800 $\mu\varepsilon$ at near to 35 kN load level (Fig. 3.12). The final specimen developed failure due to the transition mode of tensile to compression in the bond region near to failure load level of 35 kN. The specimen failure mode can be referred to in Figs. 3.13 (a) and (b).

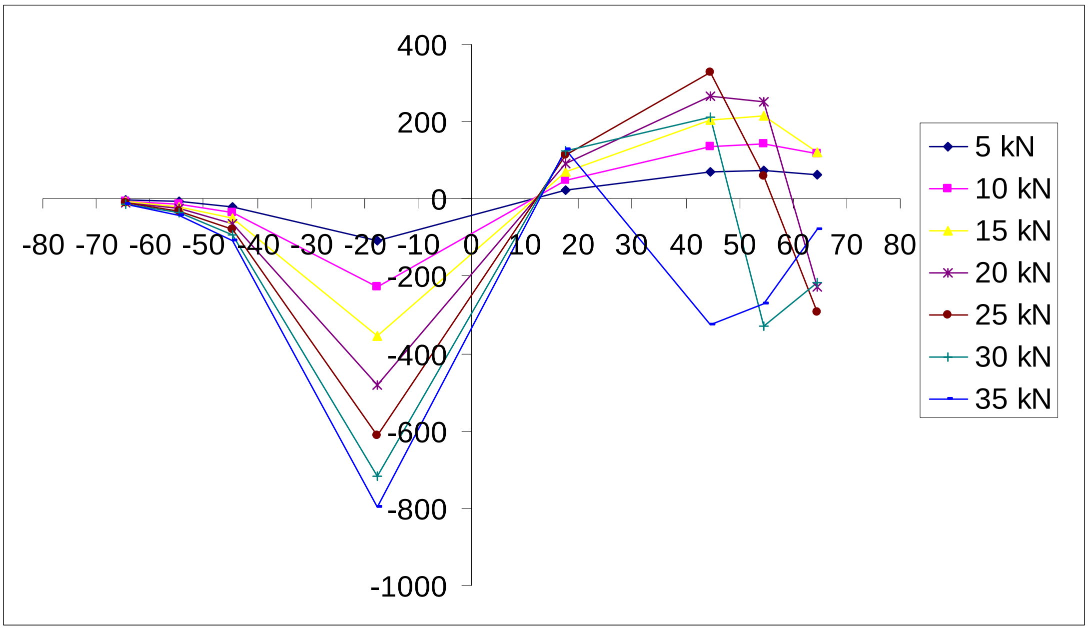

Fig. 3.11: Strain distribution along compression and tension zones for mild steel end tabs.

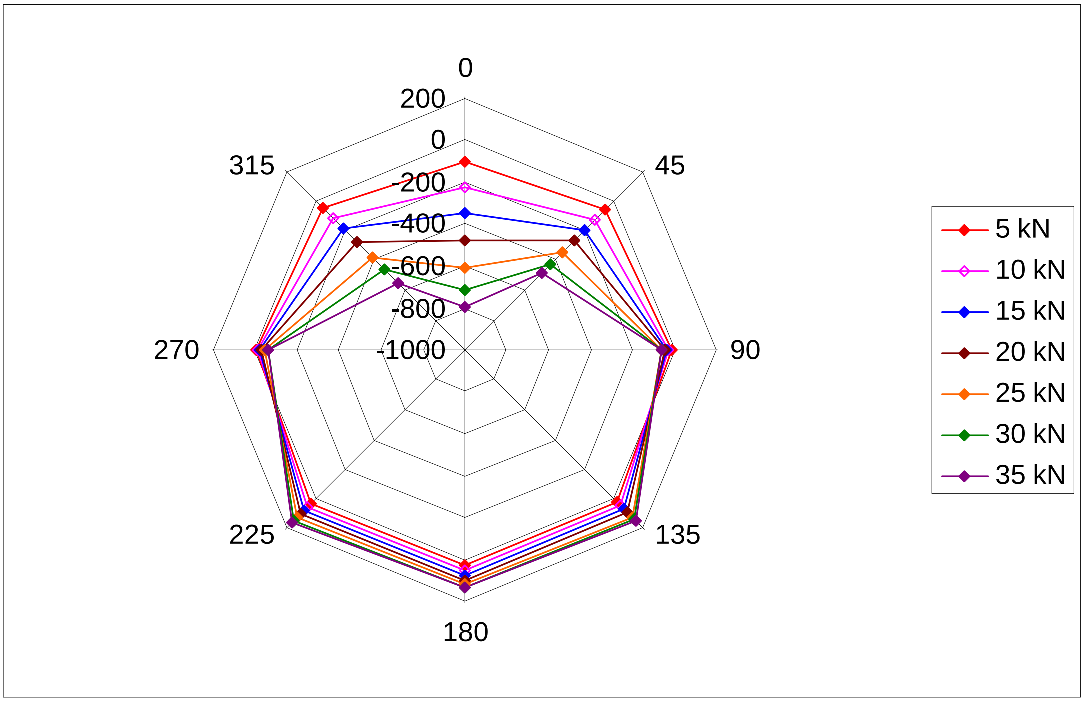

Fig. 3.12: Typical strain distribution around end tabs pinhole at various load levels

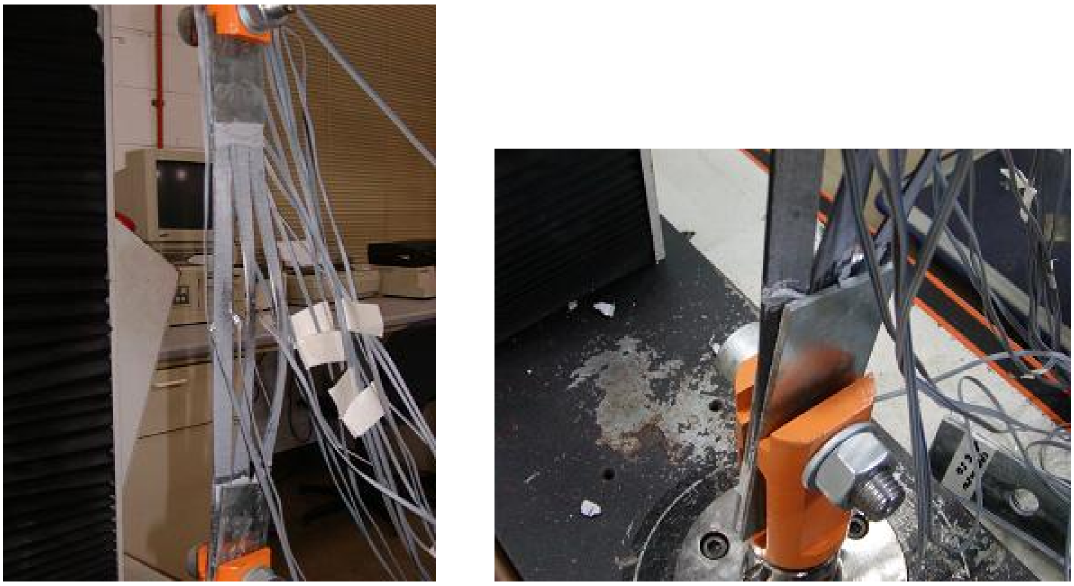

(a) (b)

Fig. 3.13: (a) The buckling effect of CFRP plate middle segment shear-out and **(b)** Close-up view of shear-out bond failure within mild steel end tabs-CFRP plate

3.6 The Final Sustainable Loads Rig Performances

The final design of the rig is shown in Fig. 3.14. Generally, the rig final design consisted of an upper constrain plate, lower constrain plate, bearing block, guide block, pin, bolts, nuts and tie rods. The loading mechanism was a 50 kN maximum capacity of mini-hydraulic jack. The load applied to the rig-specimen was measured by a load cell with the maximum capacity of 50 kN. The detailed rig-specimen's performances are described in the following sections. The loading set-up for the rig-specimen is described in detail in the following sections supported with figures and technical descriptions

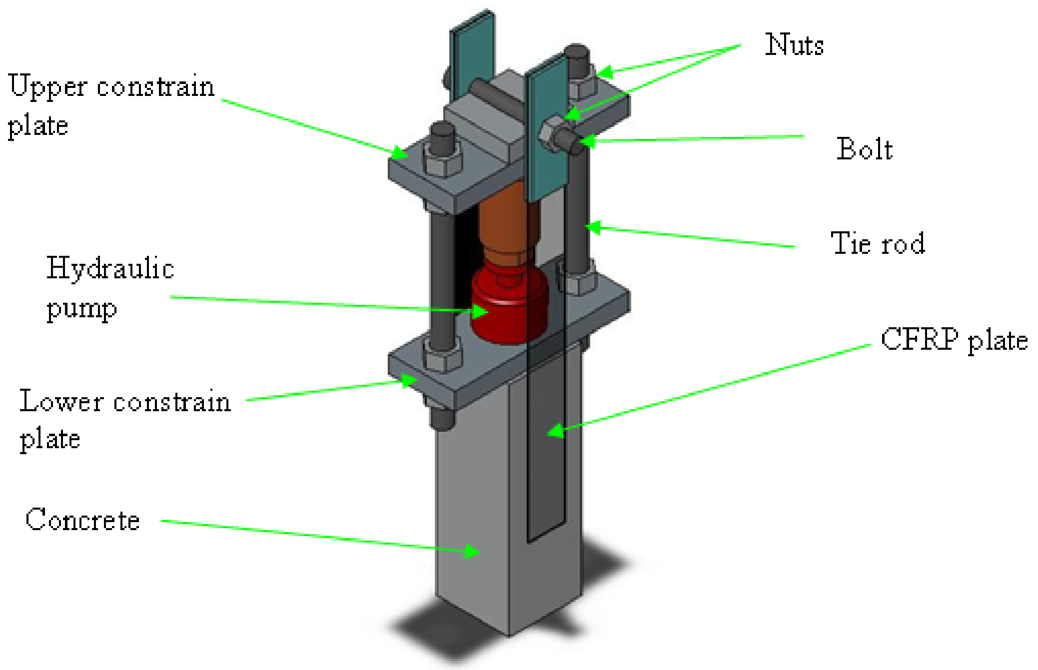

Fig. 3.14: The sustainable experimentation rig used in this study programme

3.6.1. Load Cell Calibration

The objective of the test was to calibrate the loading performance of the 50 kN maximum capacity of load cell brand TML supplied by Tokyo Sokki Kenkyujo Co. Ltd. The test was conducted by applying compression load up to the maximum loading capacity of the load cell as shown in Fig. 3.15 (a) and (b). The loading was applied using Instron 100 kN Universal Testing machine. The load produced by the machine was used as a benchmark to the output reading from the load cell. The output from load cell was read through data logger TDS-302. After reaching the maximum value, the loading on the machine was then reduced at a constant rate to zero loading capacity. From the graph shown in Fig. 3.16, it can be seen that both loading and unloading curves coincide with non-linearity almost reaching.

Fig. 3.15 (a): 50 kN load cell calibration under compression load using 100 kN Instron Universal Testing Machine

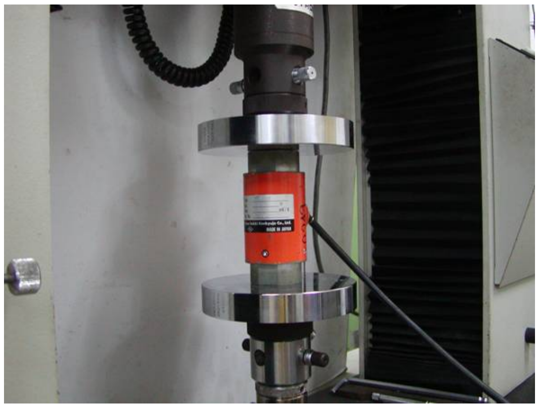

Fig. 3.15 (b): Closed up view for load cell calibration

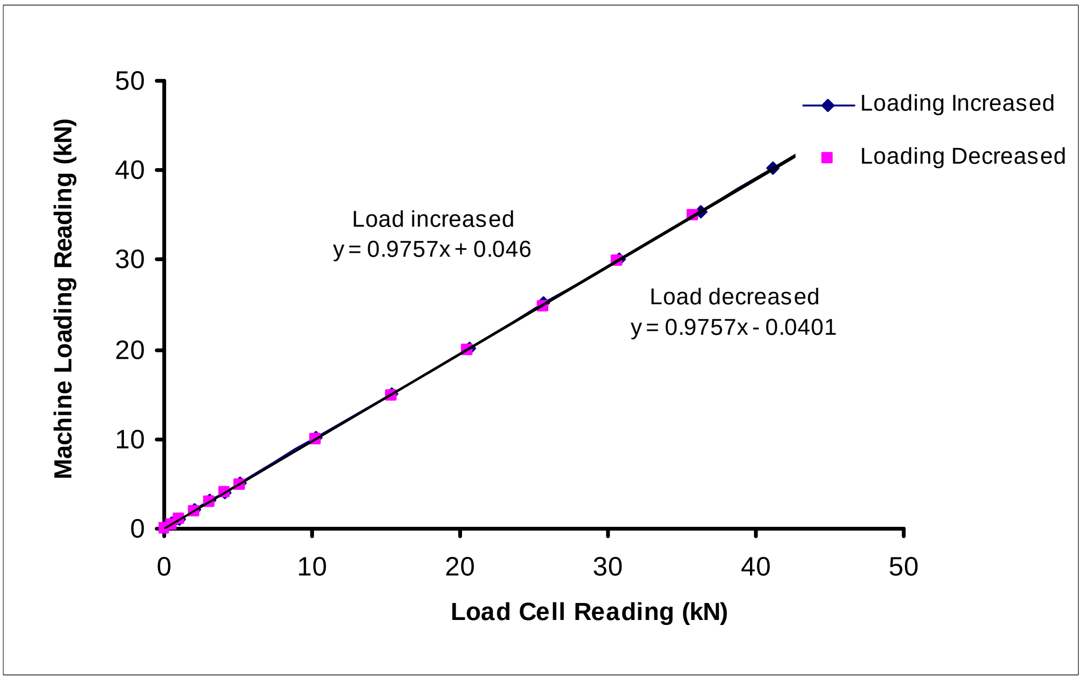

Fig. 3.16: Graph of machine load versus load cell load reading under increment and decrement of applied machine loads.

3.6.2 Rig-specimen Set-up Descriptions

The sustained loading rig-specimen set-up started with the preparation of the basic rig configuration that included height calibration. Prior to the installation of rig onto the specimen, the strain measurement on concrete prism and tie rods were taken by using standard digital Demec gauge instrument. After the completion of rig-specimen layout configuration (i.e. measurement to ensure that the rig was perfectly aligned), the 50 kN mini hydraulic pump was installed onto the lower mild steel plate. The hydraulic load applied to the rig-specimen was measured by centrally placing the load cell (load transducer) between the pump and the upper constrain plate. In order to avoid any lateral movement of the pump and transducer, circular holes depth of 3 mm depth and 50 mm in diameter were formed for both the lower and upper constrain plates. Ideally, during loading, the two high tensile steel tie rods placed on the left and right hand side of the rig-specimen should be free (not receiving any load from the pump). Both rods were only subjected to compression load just after the stress imposed on the specimen reached their specified target limit.

Nuts were used to lock or tighten the tie rod screws and to maintain the rig-specimen sustainable loads condition. Torque wrench which was initially set to the specified torque was used to lock the nuts (screws) prior to releasing the hydraulic jack load. Finally, the CFRP plate strains performances were monitored through data logger TDS-302 output. The monitoring was done every 15 minutes for the first 24 hours, followed by every 30 minutes for the next 48 hours and finally by every 24 hours for the duration of 2 months. The experimentation was conducted for three selected (control) specimens namely; BOLTALS50-OD01-1yr, BOLTALS50-OD02-1yr and BOLTALS50-OD03-1yr. The other specimens were monitored of their strains performances every 15 minutes for the duration of 24 hours before undergoing their respected experimentation exposure programme. The complete rig-specimen set-up is shown by Figs. 3.17 (a) to (k).

Fig. 3.17: (a): Setting-up stressed rig configurations

Fig. 3.17 (b): Upper and lower steel plates height calibration and measurement

Fig 3.17 (c): Inserting high tensile steel bolt into CFRP Plates-end tabs holes

Fig 3.17 (d): Installing mini hydraulic pump onto lower mild steel plate

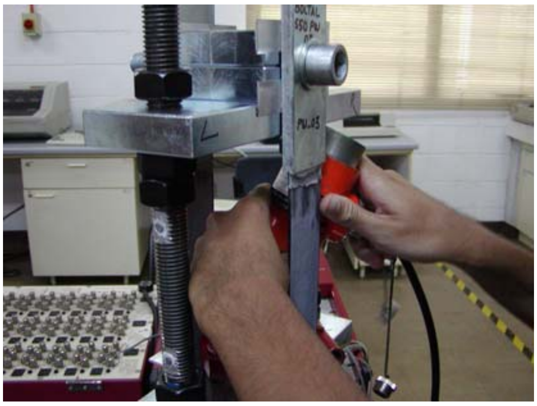

Fig. 3.17 (e): Installing load cell between the hydraulic pump and upper mild steel plate

Fig. 3.17 (f): Applying small hydraulic load to the rig-specimen for initial set-up

Fig. 3.17 (g): Increasing the hydraulic load onto the rig-specimen

Fig. 3.17 (h): Measuring the strain of concrete during pre-stressed using digital Demec Gauge instrument

Fig. 3.17 (i): Specimen left in the laboratory for strain monitoring

Fig. 3.17 (j): Strain output print-out in 30 minutes time interval for 24 hours monitoring duration

Fig. 3.17 (k): Specimens ready to be delivered in their specified exposure condition

3.6.3 Rig-Specimen Stressed Performance Results

The complete performances of the rig-specimen during pre-stressing and during sustainable load are shown in Fig. 3.18, Fig. 3.19 and Fig. 3.20 for BOLTALS50-OD01-1yr specimen. For BOLTALS50-OD02-1yr and BOLTALS50-OD03-1yr only their time-stress performances are shown as in Fig. 3.21 and Fig. 3.22.

The curve shown in Fig. 3.18 demonstrates the three stages of loading conditions experienced by the specimen, namely; stressing, tightening (locking) and applied load released or final loading condition. It can be seen that during the stressing stage, the CFRP plate strains were not in linear mode up to the final target load. This non-linearity was due to the inability of controlling the mini hydraulic pump mechanical pumping pressure at a constant rate. Therefore, it was difficult to target the final specified load imposed onto the specimen.

The second stage was the most critical stage whereby the final loads imposed into the specimen were determined by the torque that was applied to the nuts (tie rod screws). This stage needed to be completed in a fast mode and both tie rods must be in a balanced load condition. This could be verified and confirmed by monitoring the strain readings of both sides (Side A and Side B) of the CFRP plates. From Fig. 3.21, it can be seen that the difference between strain readings along the bonded length can be used as a standard benchmark to evaluate the balancing between both sides of the specimen in terms of load transfer from the applied hydraulic load. The results show that the different strain readings between each pair (i.e. reading of strain gauges at the same location, for example SG2A and SG2B etc.) for BOLTALS50-OD01-1yr ranged from 0.5 to 30% for the three loading stages and 3 to 85% for low load level condition. The same results were also recorded by BOLTALS50-OD02-1yr where the readings ranged from 0 to 20% for the three last stages and 20 to 85% for low load level condition. Finally, BOLTALS50-OD03-1yr showed a larger difference between those two specimens whereby the difference ranged from 20 to 125% for the last three stages and 7 to 19% for low load level condition. It could be said that at low to higher load levels the rig-specimen slowly adjusted their loading condition until they reached the final state of equilibrium.

In the final stage, it could be seen that strain readings dropped to the final value (i.e. less than the value just after locking) just after the applied hydraulic load had been released (i.e. load equal to zero). The rate of strains decreased along the bonded length in linear mode. The reduction was due to the loss of support provided by the hydraulic jack used during pre-stressing. Therefore, it could be seen that the rig worked successfully as designed and capable of supporting the designated stressed loads to the specimen, i.e. tensile load onto CFRP plate and compression load onto the unreinforced concrete prism.

The mechanical performance of the rig was monitored regularly through strains output from data logger TDS-302 for the duration of two months especially for the three control specimens mentioned earlier. From Fig. 3.23, Fig. 3.24 and Fig. 3.25, it can be seen that the CFRP plates strain readings were almost constant throughout the monitoring periods, i.e. after reaching their full statics equilibrium. It can be seen that the strain readings were yet not stable within the two weeks time period after applying the sustained loads. Another factor that could affect the strain performances was room condition where the specimens were kept during the time-stress monitoring. The temperature and humidity parameters had not significantly affect the stressed conditions due to very small fluctuation of the overall strain readings during the monitoring periods. Finally, it could be said that the designed stressed rig had proven its functionality of transfer tensile and compressive loads to the CFRP plate and concrete prism, respectively and sustaining the loads for longer exposure period.

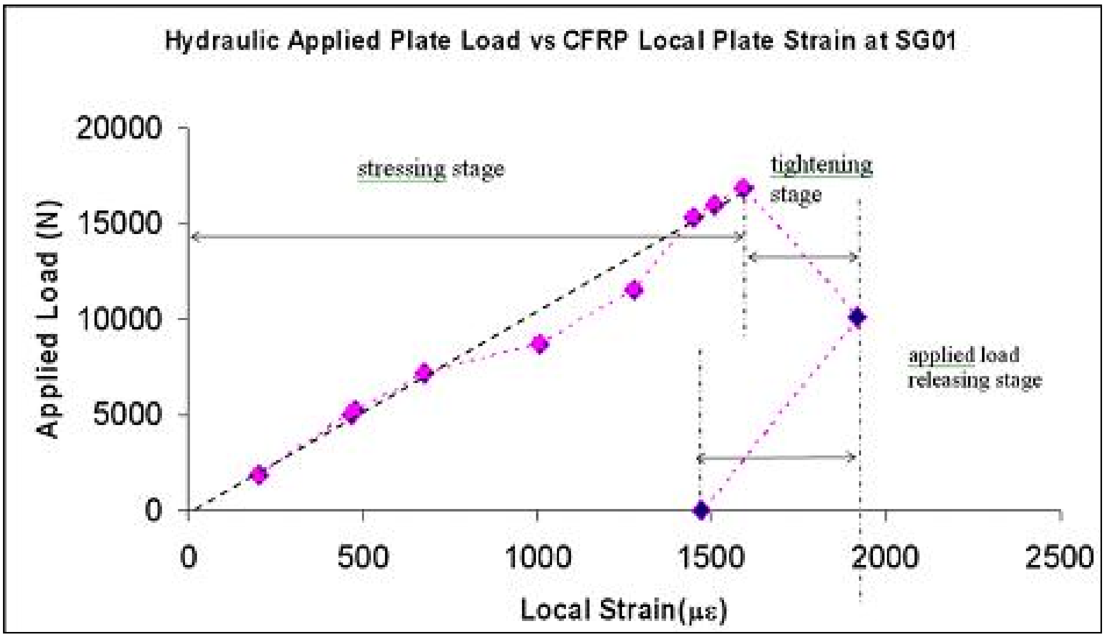

Fig. 3.18: Loading performances during stressing BOLTALS50-OD01-1yr (data refer at SG01)

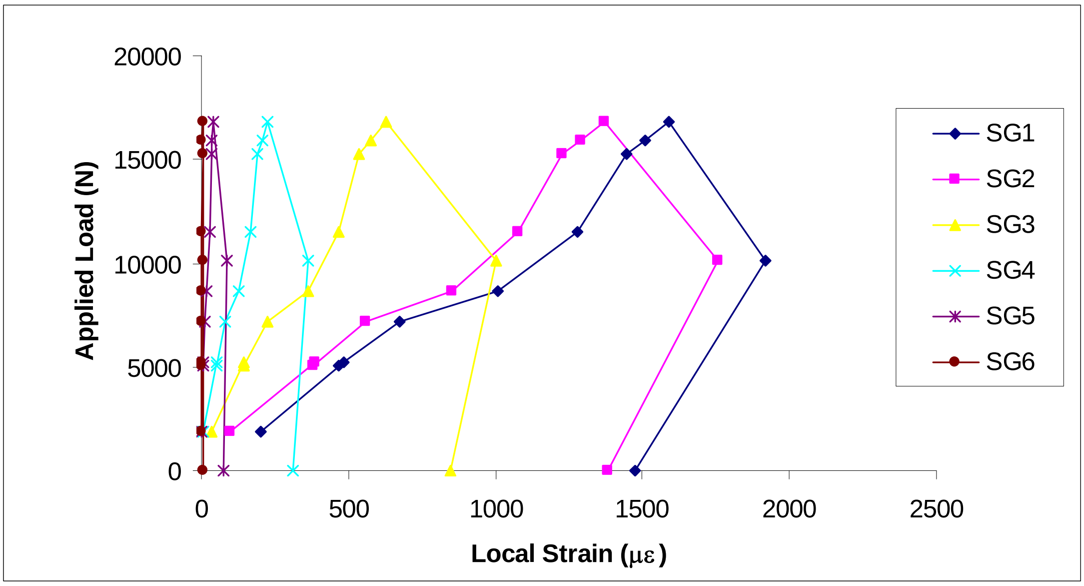

Fig. 3.19: Graph of applied hydraulic load versus CFRP plate local strains BOLTALS50-OD01-1yr

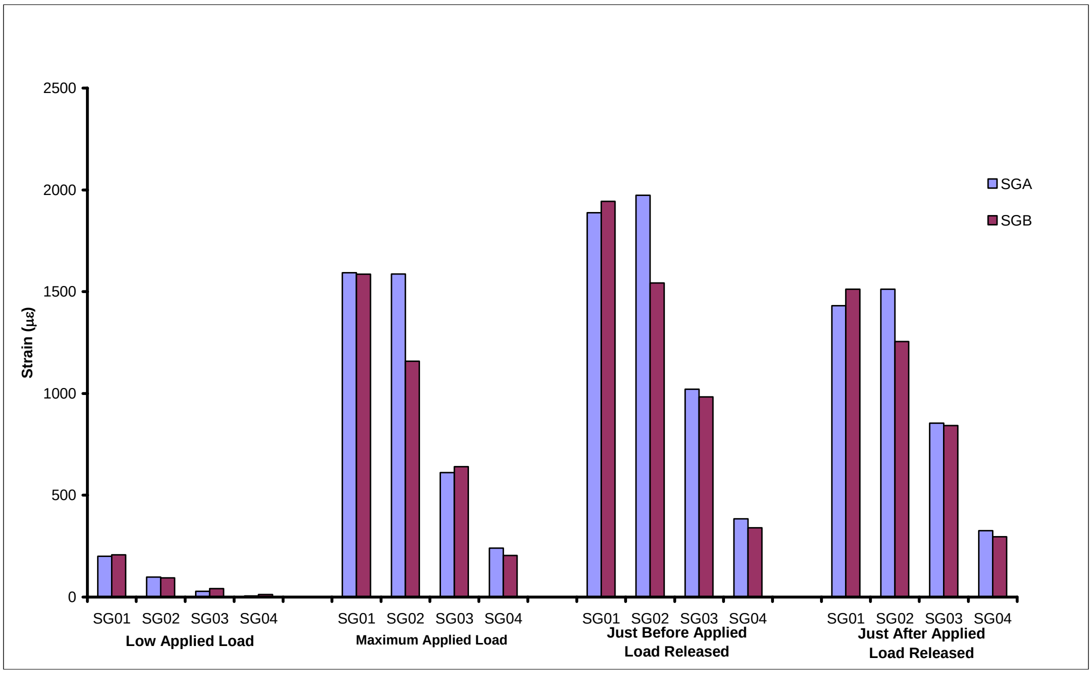

Fig. 3.20: Bar charts showing the different strain readings between Side A and Side B of CFRP plates BOLTALS50-OD01-1yr

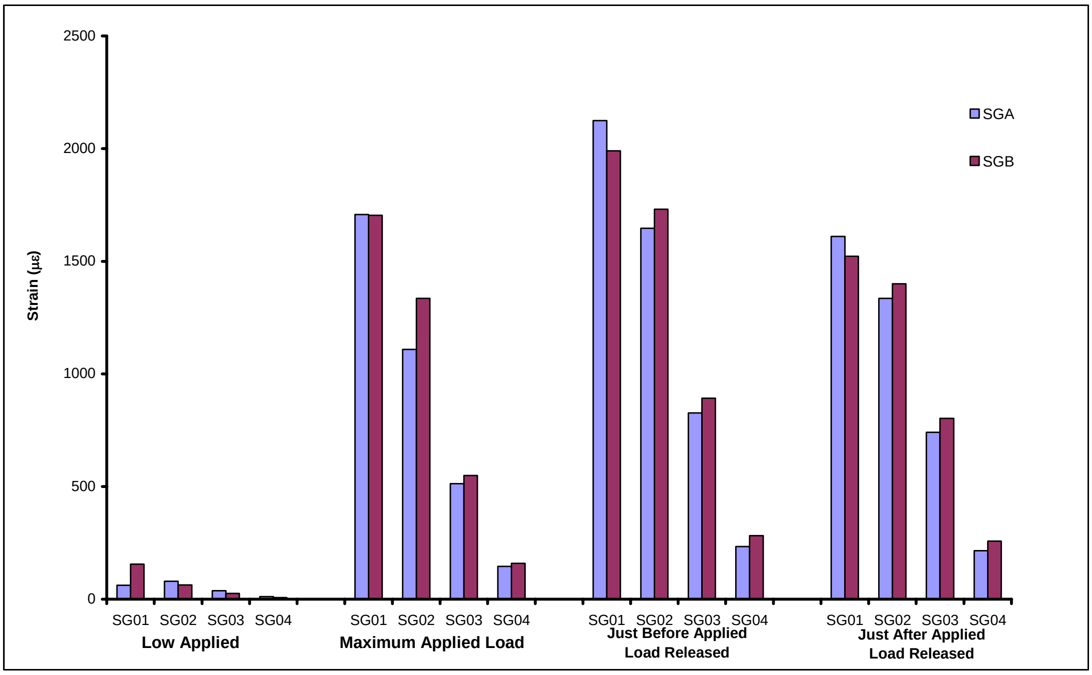

Fig. 3.21: Bar charts showing the different strain readings between Side A and Side B of CFRP plates BOLTALS50-OD02-1yr

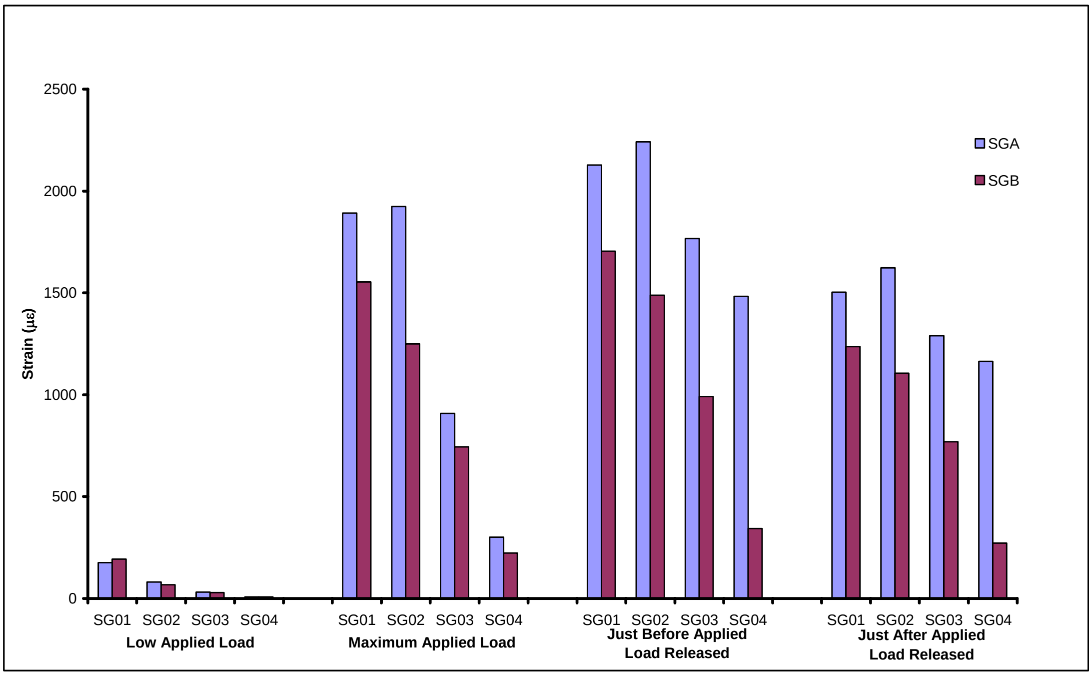

Fig. 3.22: Bar charts showing the different strain readings between Side A and Side B of CFRP plates BOLTALS50-OD03-1yr

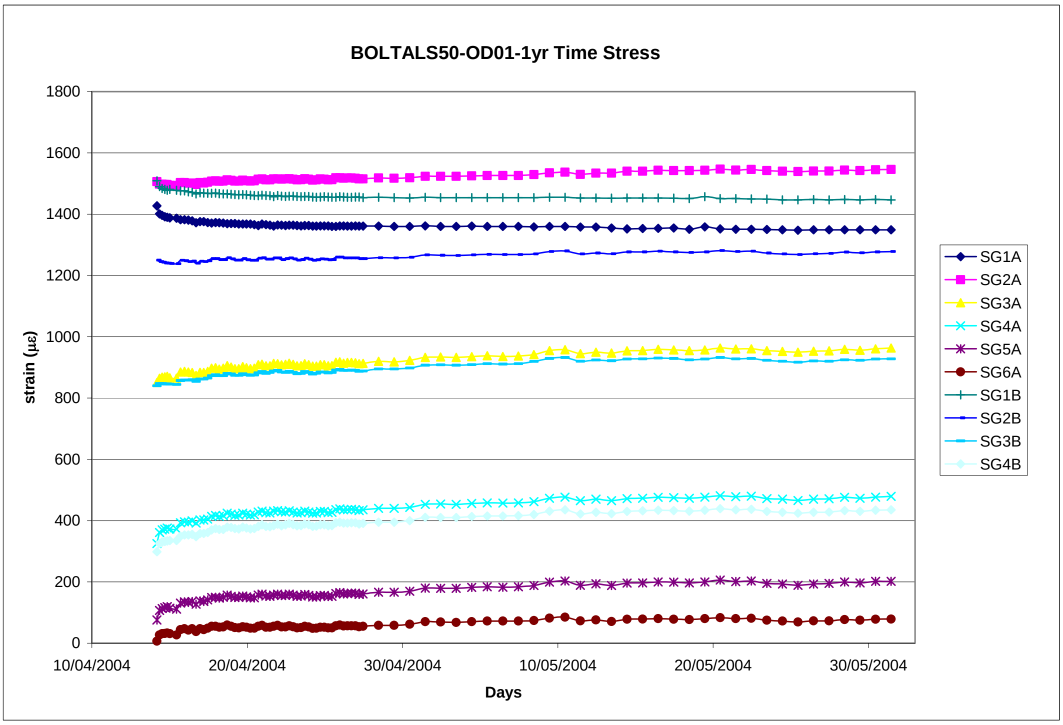

Fig. 3.23: Graph of CFRP plate local strains versus time (days) BOLTALS50-OD01-1yr Time-Stress

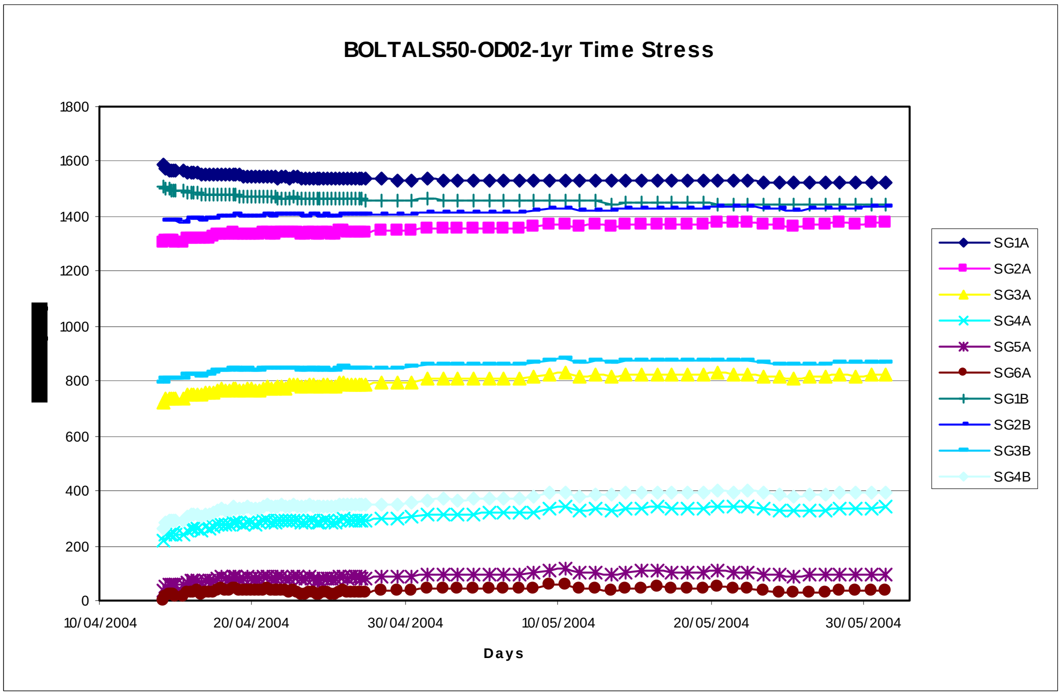

Fig. 3.24: Graph of CFRP plate local strains versus time (days) BOLTALS50-OD02-1yr Time-Stress

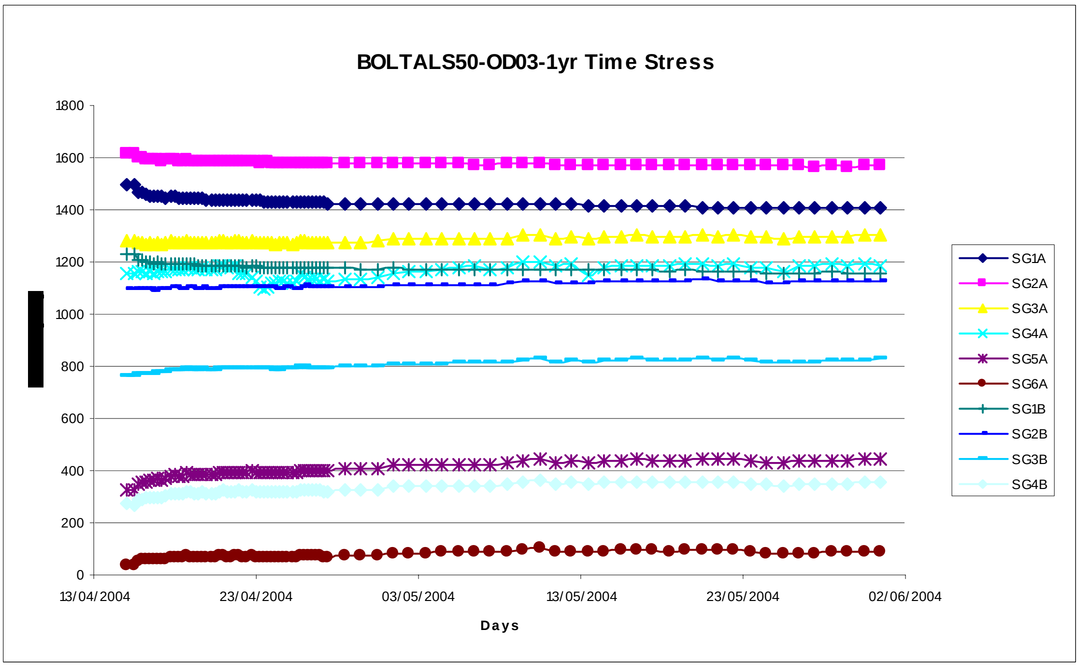

Fig. 3.25: Graph of CFRP plate local strains versus time (days) BOLTALS50-OD03-1yr Time-Stress

3.7 Conclusion

Various test methods have been developed to investigate the bond stress behaviour of FRP or steel plate-concrete bonded system since 1970's by known researchers. These include four point flexural loads test and pull-out test. Most of their studies were related to investigation into durability studies of steel and FRP plate or laminate system bonded to concrete. The studies were in conjunction with the application of FRP composites as new material system to replace steel as a material to enhance the flexural or shear capacity of reinforced concrete member. In the early age of the durability study, an investigation into the flexural performances of steel plate-concrete beam bonded system exposed to natural environmental condition under sustained load had been conducted. The researchers have used designated full mechanical rig that in such a way created a sustained four point flexural loads imposed onto a pair of externally steel plate-concrete bonded system.

There was a need for further investigation into FRP plate-concrete bonded system and bonding durability performances effect from various environmental tropical conditions. The first simple design and fabricated load sustainability test rig was successfully produced in this study programme. The rig successfully produced pull-push loading configuration on the CFRP plate-concrete prism adhesive bonded specimen. The rig was capable of transferring the load-stresses onto the specimen and sustained the load up to 50 to 65% of the control specimen ultimate failure load. The rig's load sustainability was regularly measured by digital Demec instrument during exposure periods. The reliability of the rig was technically proven even when exposed to aggressive environment such as in salt water, under wet and dry cycle condition.